Chinese Chemical Letters 35 (2024) 109638

Contents lists available at ScienceDirect

Chinese Chemical Letters

journal homepage: www.elsevier.com/locate/cclet

Unraveling the interplay of DNAzyme and interfacial factors for enhanced biosensing

Yiyang Shen[a,b,1], Zhen Zhang[a,1,*], Ruyi Liang[b], Tongbo Wu[b,*]

[a] The First Affiliated Hospital, and College of Clinical Medicine of Henan University of Science and Technology, Luoyang 471003, China
[b] School of Pharmacy, Tongji Medical College, Huazhong University of Science and Technology, Wuhan 430030, China

ARTICLE INFO

Article history:
Received 27 December 2023
Revised 5 February 2024
Accepted 7 February 2024
Available online 12 February 2024

Keywords:
DNAzyme
Gold nanoparticles
Interfacial factor
Multiple modulation functions
miRNA detection

ABSTRACT

Deoxyribozyme (DNAzyme) and its substrate hybridization are crucial for achieving desirable detection performance in the DNAzyme coupling nanomaterial biosensor system. However, interfacial factors such as electrostatic repulsion, steric hindrance, and nonspecific adsorption from gold nanoparticles make this hybridization process complicated and challenging. Moreover, the DNAzyme structure changes with different application purposes, which might affect the DNAzyme and substrate's connection. Few studies have focused on the interplay of DNAzyme and interfacial factors in the biosensor field. In this work, three types of DNAzyme variants were designed, and their biosensor performance rules were studied and summarized with the synergistic effect of interfacial factors. Additionally, corresponding biosensor applications, such as multiple modulation functions and miRNA detections, were constructed based on the distinct principles of DNAzyme variants.

Since the selection of the first Pb^{2+}-dependent deoxyribozyme (DNAzyme) in 1994 [1], various types of DNAzymes have constantly emerged, gaining attention in molecular biology due to their integral catalytic activity and programmability [2]. DNAzymes with cleavage activity bind to their corresponding substrates and hydrolyze them. The DNAzyme sequence generally consists of two parts: the recognition arm sequence, which hybridizes with the substrate [3–5], and the catalytic core sequence, which processes the catalytical activity [6–8]. Additionally, the catalytical activity activation of DNAzyme also requires cofactors such as K^+, Na^+, Pb^{2+}, Mg^{2+}, and Mn^{2+} [9,10]. Modulating the activity of DNAzymes can be achieved by adjusting or redesigning the above three elements involved in the DNAzyme system. This enables different functions in various fields, such as biosensors, bioimaging, and drug delivery [11,12].

Nanomaterials, especially DNA-functionalized nanomaterials, have attracted the attention of researchers due to their superior sensing performance [13–15]. Gold nanoparticles (AuNPs) have emerged as a helpful biosensor material with their easy DNA modification and extensive fluorescence quenching capabilities [16,17]. The advantages of DNAzyme and DNA-AuNPs can be combined with the simple base pairing principle for constructing the amplified signal detection platform [18]. In this platform, the fluorophore-labeled DNAzyme substrates are modified on the surface of AuNPs (abbreviated as DS-AuNPs) through solid gold-sulfur bonds [19] or polyadenine [20,21]. The substrates can be subsequently hydrolyzed by DNAzyme, resulting in a detectable signal [22]. The excellent detection performance of this platform heavily relies on the successful hybridization of DNAzyme to DS-AuNPs.

Unfortunately, interfacial factors such as nonspecific adsorption [23], electrostatic repulsion [24], and steric hindrance [25] significantly affect the connection of DNAzyme to DS-AuNPs. Our previous research demonstrated that artificially extending the DNAzyme recognition arm negatively impacted its cleavage activity towards DS-AuNPs compared to the normal DNAzyme, which was attributed to interfacial factors [26]. However, our investigation only focused on the one-end extension type of DNAzyme variants, which may not meet the diverse demand for DNAzyme-based biosensors. Additionally, we did not discuss the interaction principle between DNAzyme and DS-AuNPs. Therefore, it is essential to comprehensively explore the relationship between different types of DNAzyme variants and the interface factors induced by DS-AuNPs for multiple application purposes.

In this work, we designed a series of 8-17E DNAzyme variants with versatile recognition arm extension structures (Scheme 1A). The detailed DNA sequences are listed in Table S1 (Supporting information). Scheme 1B briefly illustrated the synergistic effect of

* Corresponding authors.
E-mail addresses: zhangzhen9009@163.com (Z. Zhang), wutongbo@hust.edu.cn (T. Wu).
[1] These authors contributed equally to this work.

https://doi.org/10.1016/j.cclet.2024.109638
1001-8417/

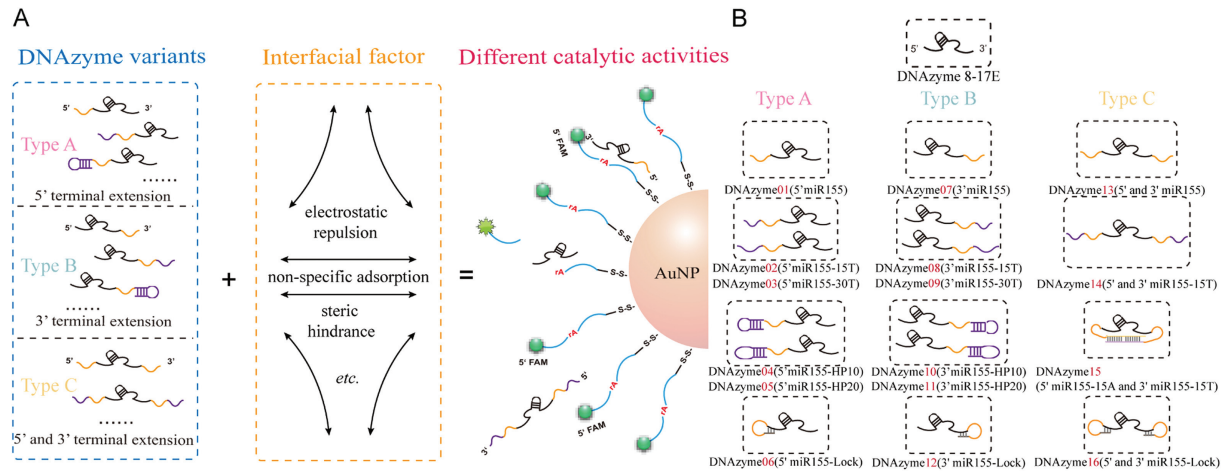

Scheme 1. (A) The schematic diagram of the synergistic effect of the DNAzyme nonfunctional structural changes and interfacial factors on DNAzyme activity. (B) The series of 8-17E DNAzyme variants with versatile recognition arm extension structures.

DNAzyme variants and interfacial factors on the detection system signal output. We first immobilized the substrate of the 8-17E DNAzyme with 5′ terminal carboxyfluorescein (FAM) and 3′ terminal sulfhydryl modification (HS-) modification onto the AuNPs, forming DS-AuNPs. The terminal HS- in the single-stranded DNA (ssDNA) is widely used to connect ssDNA with AuNPs to form DNA-functionalized AuNPs through the Au-S bond. We also added a 13-nt poly-thymine spacer in the AuNPs substrate to enhance its accessibility to the DNAzyme [26,27]. In the initial state, FAM fluorescence was quenched by AuNPs. Once the DNAzyme variant hybridizes with the substrate labeled on the AuNPs, it will cleave the substrate with the help of the cofactor Mn^{2+}, releasing the FAM-modified substrate fragment and restoring the FAM fluorescence. Simultaneously, the DNAzyme variant could be reused to hybridize another substrate, resulting in an amplified fluorescence signal. The rate of fluorescence increase of the system can reflect the catalytic activities of different DNAzyme variants. Since the catalytic core and the recognition arm sequences of these DNAzyme variants were identical, their catalytic performance differences were due to the synergistic effects of the nonfunctional region in the DNAzyme and the interfacial factors on the DS-AuNPs. Based on the regulation principles of DNAzyme variants, the corresponding biosensor applications, such as direct miRNA response, multiple modulation functions, and enzyme-aided miRNA detection, were constructed.

The newly designed DNAzyme variants were classified into three categories (Scheme 1B): Type A included variants with 5′ extensions (DNAzyme 01 to 06 and 17 to 22), Type B included variants with 3′ extensions (DNAzyme 07 to 12 and 23 to 28), and Type C included variants with both 3′ and 5′ extensions (DNAzyme 13 to 16). To assess their potential for biosensing applications, the nonfunctional region sequences in the DNAzyme (the orange line of DNAzyme variants in Scheme 1) were designed to complement miRNA-155 or miRNA-21. We selected five DNAzyme variants from the three categories to validate their feasibility and evaluated their catalytic activities on DS-AuNPs by calculating the relative rate of fluorescence increase (R) (Fig. 1). R was calculated as V/V_0, where V is the rate of fluorescence increase induced by the DNAzyme variant, and V_0 is the rate of fluorescence increase induced by the original 8-17E DNAzyme. As depicted in Fig. S1 (Supporting information), all selected DNAzyme variants showed limited catalytic activities towards DS-AuNPs ($R < 1$), which was different from their performance towards free DNAzyme substrates in solution labeled with FAM and the quencher (free substrate in Table S1). These results suggested a negative effect on the DNAzyme activity under the synergistic effects of interfacial factors and the nonfunctional

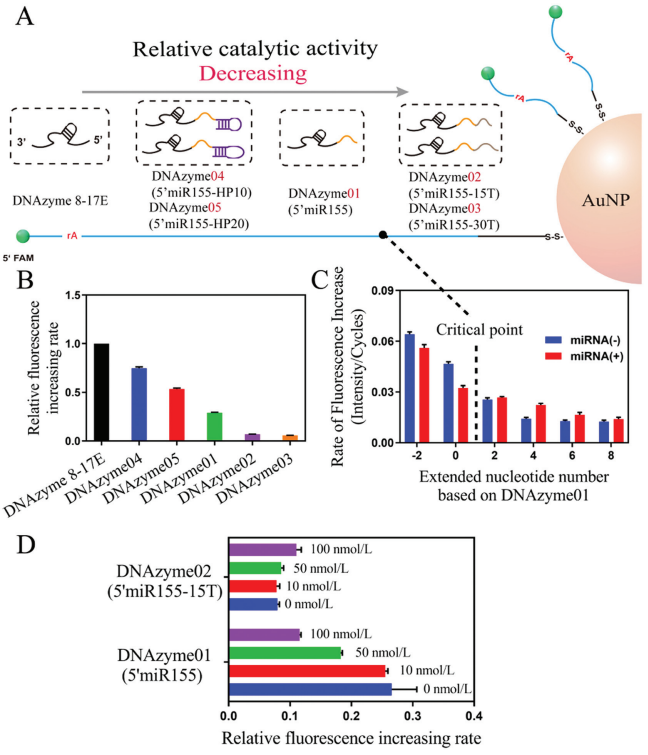

Fig. 1. (A) The comprehensive effect on the cleaving activity of 5′ extended DNAzyme variants based on structural transformation and interfacial factor. (B) The relative fluorescence increasing rate of DNAzyme variants with different 5′ extension structures. (C) The relationship between the relative fluorescence increasing rate and the extended nucleotide number of DNAzyme variants with or without miRNA-155 (miR155) addition. The critical point was also shown. (D) The relative fluorescence increasing rate produced by DNAzyme01 and DNAzyme02 after adding 0, 10, 50, and 100 nmol/L miR155. Error bars: mean ± standard deviation (SD) ($n = 3$).

region of DNAzyme variants. Fig. S1 showed the relative activities of all DNAzyme variants used in this work for free substrate in solution. We investigated and analyzed the activities of these DNAzyme variants on DS-AuNPs in subsequent sections, respectively.

We first investigated the activity of five Type A DNAzyme variants (DNAzyme 01 to 05 in Fig. 1A). DNAzyme01 extended 23 bases complementary to miRNA-155 at the 5′-end of DNAzyme

8-17E. DNAzyme02 and DNAzyme03 extended 15 or 30 thymine bases at the 5′-end of DNAzyme01. DNAzyme04 and DNAzyme05 extended a hairpin structure with a 10-basepair (10-bp) stem and a 10-nt or 20-nt polythymine (poly-T) loop. As shown in Fig. 1B, all these five DNAzyme variants had smaller activity for DS-AuNPs than the original 8-17E DNAzyme (DNAzyme0). Interestingly, DNAzyme02/03′s activity was much smaller ($R = 0.058$ and 0.069) than DNAyzme01's activity ($R = 0.291$), and DNAzyme04/05′s activity was bigger ($R = 0.748$ and 0.535). While for free substrate in the solution, R for these DNAzyme variants ranged from 0.776 to 1.180 (Fig. S2 in Supporting information), which was quite different from DS-AuNPs. These results suggested that the interfacial factors on AuNPs significantly affect the activity of DNAzyme, and the extended ssDNA and hairpin structure had different interactions with the interfacial factors. Next, we focused on the discussion about the DNAzyme activity towards DS-AuNPs. With more extended ssDNA bases, the R was smaller, which was in accordance with our previous results, indicating that the increased nonspecific adsorption and electrostatic repulsion decreased the chance for DNAzyme to reach the AuNPs surface to cleave the substrate on it. With the extended hairpin structure, although the nonfunctional region also increased, R increased compared to DNAzyme01. We speculated that the steric hindrance of the hairpin structure impedes the accessibility of the 5′-end of DNAzyme04/05 to the DS-AuNPs surface. Thus, the nonspecific adsorption effect was reduced compared with DNAzyme01. DNAzyme05 had ten more bases in the hairpin loop than DNAzyme, so the nonspecific adsorption effect was bigger, and the activity was more minor.

To further examine the influence of the nucleotides extended at the 5′-end of DNAzyme01 without secondary structure, we designed a series of DNAzyme variants DNAzyme01/nT, where n indicates the number of extended thymine bases and ranges from −2 to 28 (sequences in Table S1). We found that increasing the extended T bases led to lower DNAzyme catalytic activity, as indicated by the blue columns in Fig. 1C and the blue points in Fig. S3 (Supporting information). This was in accordance with the hypothesis that more extended T bases cause more nonspecific adsorption. Then, we used miRNA-155 to regulate the system's interfacial factors. The addition of miRNA reduced DNAzyme's nonspecific adsorption effect while increasing the electrostatic repulsion and steric hindrance effect on DS-AuNPs. Red columns depicted the effects of miRNA addition on the activity of DNAzyme variants in Fig. 1C and red points in Fig. S3. When $n > 2$ in DNAzyme01/nT variants, the presence of miRNA exhibited a positive effect, and the blue column height was shorter than the red column in Fig. 1C. Conversely, when $n < 2$ in DNAzyme01/nT variants, the addition of miRNA decreased the activity of the DNAzyme variants, and the red column height was shorter than the blue column in Fig. 1C. We hypothesized that a critical point may be shown in Fig. 1C for the domination of the interfacial factors. The DNAzyme variants are located further to the right with more extended bases. On the right side of the critical point, nonspecific adsorption dominates the interfacial factors. On the left side of the point, electrostatic repulsion and steric hindrance dominate the interfacial factors. Thus, adding miRNA caused a positive or negative regulation effect for different DNAzyme variants.

Subsequently, we examined the biosensor potential of DNAzyme01 (a DNAzyme variant on the left side of the critical point) and DNAzyme02 (a DNAzyme variant on the right side of the critical point) by introducing different concentrations of miRNA-155 (Fig. 1D). As anticipated, increasing the concentration of miRNA-155 resulted in an increase or decrease in DNAzyme activity. Most Type A DNAzyme variants exhibited similar trends in catalytic rates (Figs. S4A–E in Supporting information). Interestingly, DNAzyme04 and 05 with hairpin loops of different bases and DNAzyme06 with locked recognition areas showed weaker

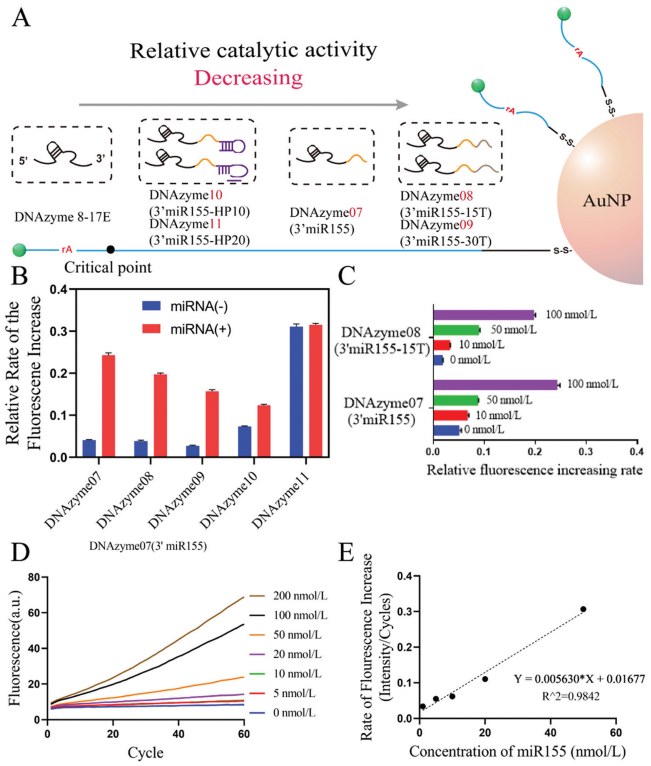

Fig. 2. (A) The comprehensive effect on the cleaving activity of 3′ extended DNAzymes based on structural transformation and interfacial factor. (B) The relative fluorescence increasing rate of DNAzyme variants with different 3′ extension structures. (C) The relative fluorescence increasing rate produced by DNAzyme 07 and DNAzyme08 after adding 0, 10, 50, and 100 nmol/L miR155. (D) The fluorescence response produced by DNAzyme 07 after adding miR155 on DS-AuNPs. (E) The relationship between the concentration of added miR155 and the rate of fluorescence increase. Error bars: mean ± SD ($n = 3$).

regulation potential than DNAzyme with simply extended regions. The structure and restricted area explained the phenomenon. After adding miRNA-155, the DNA-RNA duplex formed at the 5′-end compared to the previous structures with a bulky hairpin loop or restricted functional area. No significant change (Figs. S4F–H in Supporting information) showcased a similar comprehensive effect produced by bulky structures, including hairpin loops, DNA-RNA duplexes, and locked recognition arm sequences.

We next investigated the activity of five Type B DNAzyme variants (DNAzyme07 to 11 in Fig. 2A). DNAzyme07 extended 23 bases complementary to miRNA-155 at the 3′-end of DNAzyme 8-17E. DNAzyme08 and DNAzyme09 extended 15 or 30 thymine bases at the 5′-end of DNAzyme07. DNAzyme10 and DNAzyme11 extended a hairpin structure with a 10-base pair (10-bp) stem and a 10-nt or 20-nt poly-T loop. The trend of the Type B DNAzyme variants' activity (column in Fig. 2B) was similar to that of the Type A DNAzyme variants, though the R was smaller for a similar design. We speculated that for Type B DNAzyme variants if the extended bases at the 3′-end adsorbed to the DS-AuNPs surface, the direction of the DNAyzme became 5′ to 3′, which was the same as the substrate on AuNPs and made it more difficult to hybridize with the substrate. Meanwhile, the direction for Type A DNAzyme variants was still 3′ to 5′ after adsorption. For the Type B DNAzyme variants, adding miRNA-155 resulted in a positive regulatory trend (red column in Fig. 2C and Fig. S5 in Supporting information). These results suggested that all the tested Type B DNAzyme variants were on the critical point's right side. Adding miRNA-155 decreased the nonspecific adsorption and increased the activity of DNAzyme variants. The difference between

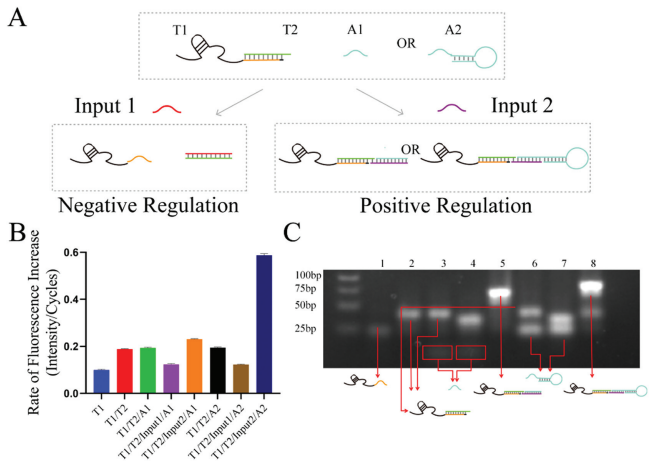

Fig. 3. (A) Schematic illustration of structural regulatory strategy and the effect of different inputs and bulky strands. (B) The rate of fluorescence increase for different complexes of DNAzyme and other strands. (C) Gel electrophoresis of the complex with different inputs. Lane 1: T1. Lane 2: T1/T2. Lane 3: T1/T2/A1. Lane 4: T1/T2/Input1/A1. Lane 5: T1/T2/Input2/A1. Lane 6: T1/T2/A2. Lane 7: T1/T2/Input1/A2. Lane 8: T1/T2/Input2/A2. Error bars: mean ± SD ($n = 3$).

Type A and Type B DNAzyme variants could be attributed to the appropriate orientation between the DNAzyme variants and their substrates, as discussed above. Still, for the DNAzyme variants with hairpin structure, both Type A and Type B DNAzyme variants had weak regulation capability. We also tested the universality of the Type B DNAzyme variants, and similar effect was produced by DNAzyme23-27 which had the extended sequence complemented to miRNA-21 at the 3′ end (Fig. S6 in Supporting information). Biosensor applications were constructed using DNAzyme07 as an example. Notably, a good linear relationship was observed between the concentration of miRNA-155 (ranging from 5 nmol/L to 50 nmol/L) and the rate of fluorescence increase in the system (Figs. 2D and E).

Multiple modulation functions involving positive and negative regulation were developed based on the regulatory principles of DNAzyme variants on DS-AuNPs (Fig. 3A). 8-17E DNAzyme variant T1 was designed with 3′-end extension of nonfunctional sequences, which are complementary to an ssDNA T2. T1/T2 complex with the assistant strand (A1 or A2) in the reaction system could be positively or negatively regulated with different inputs (Input1 or Input2). With the addition of Input1, T2 and Input1 formed a stable dsDNA through a toehold-mediated strand displacement. Compared to the original T1/T2 complex, the newly exposed T1 exhibited stronger nonspecific adsorption to DS-AuNPs, resulting in a negative regulatory effect (Fig. 3B). When Input2 is introduced, T1/T2 and assistant strand could form T1/T2/Input2/A1 or T1/T2/Input2/A2 complex with strand hybridization. In these complexes, nonspecific adsorption is blocked better than T1/T2, and the steric hindrance at the 3′-end affects the orientation of T1 to be more accessible to the substrate. Thus, Input2 showed a positive regulation effect (Fig. 3B). Both the A1 and A2 positively influenced the catalytic activity of the DNAzyme variant on DS-AuNPs. Notably, the stem-loop structure in A2 provided stronger steric hindrance and exhibited a more obvious regulatory effect (lane 8 in Fig. 3B) compared to A1 (lane 5 in Fig. 3B). Gel electrophoresis (Fig. 3C) verified the formation of the complex with different inputs so that different signals were produced. The bidirectional moderating effects of interface factors could also be used in biological logic circuits. Desirable outputs could be obtained for different inputs by simply regulating the interface factors, which may be further used to realize complicated biological networks.

We next investigated the activity of five Type C DNAzyme variants (DNAzyme 13 to 16 in Fig. S7 in Supporting information). DNAzyme13 extended 23 bases complementary to miRNA-155 at both 5′- and 3′-ends of DNAzyme01. DNAzyme14 extended 15 thymine bases at 5′- and 3′-ends of DNAzyme13. DNAzyme15 extended 15 adenine bases at the 5′-end and 15 thymine bases at the 3′-end of DNAzyme13. DNAzyme16 had 7 bases at both 5′- and 3′-ends of DNAzyme01, complementary to the recognition areas at the 5′- and 3′-sides of the catalytic core sequence. With both end extensions, the nonspecific adsorption effect was greater, and the Type C DNAzyme variants could hardly react with DS-AuNPs, showing a good background in positive regulation. However, the positive regulation effect was small with the addition of miRNA-155, as shown in Fig. S8 (Supporting information). Maybe the rigid duplex structure at both ends significantly decreased the DNAzyme activity. So, we introduced duplex-specific nuclease (DSN) to enable the release of the original 8-17E DNAzyme and reuse miRNA-155 (Fig. S9A in Supporting information). The influence of miRNA-155 and DSN addition on different Type C DNAzyme variants is presented in Fig. S9B (Supporting information). Among them, DNAzyme16 exhibited the most effective regulatory capability due to its double-blocked structure, which resulted in a lower background signal.

In conclusion, this study investigated the comprehensive effects of DNAzyme variants with different nonfunctional structures and the changes in interfacial factors between DNAzyme variants and DS-AuNPs. The regulatory principles of these DNAzyme variants were summarized and applied to construct different biosensors. This work provided a deeper understanding of the interplay between interfacial factors and DNAzyme variants, suggesting that the interfacial factors should be prudently considered when designing biosensors involving the hybridization of DNA-functional nanomaterials and DNA oligos. The regulatory principles of interfacial factors could be used to construct diverse biosensor detection systems or biological logic circuits and expanded to the interaction between DNAzyme and other nanomaterials.

Declaration of competing interest

The authors declare that they have no known competing financial interests or personal relationships that could have appeared to influence the work reported in this paper.

Acknowledgments

This study was financially supported by the National Natural Science Foundation of China (Nos. 82172372 and 82302651) and the Training Program of Innovation and Entrepreneurship for Undergraduates of Hubei Province (No. S202210487267).

Supplementary materials

Supplementary material associated with this article can be found, in the online version, at doi:10.1016/j.cclet.2024.109638.

References

[1] R.R. Breaker, G.F. Joyce, Chem. Biol. 1 (1994) 223–229.
[2] I. Cozma, E.M. McConnell, J.D. Brennan, Y. Li, Biosens. Bioelectron. 177 (2021) 112972.
[3] D.Y. Wang, D. Sen, J. Mol. Biol. 310 (2001) 723–734.
[4] S. Xu, Y. Liu, S. Zhou, Q. Zhang, N.K. Kasabov, Biomolecules 11 (2021) 1797.
[5] H. Peng, X.F. Li, H. Zhang, X.C. Le, Nat. Commun. 8 (2017) 14378.
[6] J. Gao, N. Shimada, A. Maruyama, Biomater. Sci. 3 (2015) 716–720.
[7] K. Yang, J.C. Chaput, J. Am. Chem. Soc. 143 (2021) 8957–8961.
[8] W. Li, H. Wang, S. Yang, et al., Anal. Chem. 94 (2022) 2827–2834.
[9] Z. Chen, Q. He, M. Zhao, et al., Microchim. Acta 184 (2017) 4015–4020.
[10] T. Nakama, Y. Takezawa, D. Sasaki, M. Shionoya, J. Am. Chem. Soc. 142 (2020) 10153–10162.

[11] M. Liu, D. Chang, Y. Li, Acc. Chem. Res. 50 (2017) 2273–2283.
[12] R.J. Lake, Z. Yang, J. Zhang, Y. Lu, Acc. Chem. Res. 52 (2019) 3275–3286.
[13] T. Xiao, J. Huang, D. Wang, T. Meng, X. Yang, Talanta 206 (2020) 120210.
[14] M. Giersig, P. Mulvaney, Langmuir 9 (1993) 3408–3413.
[15] Y. Fang, Y. Wang, L. Zhu, et al., Chin. Chem. Lett. 34 (2023) 108092.
[16] B. Chen, L. Mei, R. Fan, et al., Chin. Chem. Lett. 32 (2021) 1775–1779.
[17] Y. Liu, T. Li, G. Yang, et al., Chin. Chem. Lett. 33 (2022) 1913–1916.
[18] W. Deng, J.Y. Xu, H. Peng, et al., Biosens. Bioelectron. 217 (2022) 114704.
[19] M. Cárdenas, J. Barauskas, K. Schillén, et al., Langmuir 22 (2006) 3294–3299.
[20] D. Li, Q. Wen, Y. Zhou, et al., Anal. Methods 15 (2023) 626–630.
[21] J. Xu, Q. Tang, R. Zhang, et al., J. Pharm. Anal. 12 (2022) 808–813.
[22] Z. Zhang, Y. Hu, W. Yuan, et al., Anal. Chem. 93 (2021) 9939–9948.
[23] F. Zhang, S. Wang, J. Liu, Anal. Chem. 91 (2019) 14743–14750.
[24] H. Li, L. Rothberg, Proc. Natl. Acad. Sci. U. S. A. 101 (2004) 14036–14039.
[25] Y. Takeda, T. Kondow, F. Mafuné, J. Phys. Chem. C 112 (2008) 89–94.
[26] Y. Hu, Z. Zhang, W. Zhang, et al., Chin. Chem. Lett. 33 (2022) 3026–3030.
[27] Y. Tu, J. Wu, K. Chai, et al., Talanta 260 (2023) 124649.